Oxide traps in Si-SiO_2 structures characterized by tunnel emission with deep-level transient spectroscopy

D. Vuillaume
Laboratoire de Physique des Solides, Institut Supérieur d'Electronique du Nord, 41 Boulevard Vauban, 59046 Lille Cédex, France

J. C. Bourgoin
Groupe de Physique des Solides de l'Ecole Normale Supérieure, Université de Paris VII, Tour 23, 2 place Jussieu, 75251 Paris Cédex 05, France

M. Lannoo
Laboratoire de Physique des Solides, Institut Supérieur d'Electronique du Nord, 41 Boulevard Vauban, 59046 Lille Cédex, France

(Received 16 October 1985; revised manuscript received 18 February 1986)

The possibility of characterizing the traps of the oxide layer near the Si/SiO_2 interface using deep-level transient spectroscopy (DLTS) is pointed out. By use of the so-called saturating-pulse DLTS, an unusual increase of the DLTS spectrum is observed. This behavior is interpreted by taking into account tunneling emission from oxide traps situated near the silicon dioxide—silicon interface (≈ 10 to 30 Å). By introducing a model for the derivation of the DLTS signal amplitude, we show here how the deconvolution between interface states and oxide traps is allowed. Then, from the experimental study of the filling kinetics the concentration of these oxide traps is obtained ($\approx 10^7$ to 10^8 cm^{-2}) as well as their associated tunneling capture cross section ($\approx 10^{-22}$ to 10^{-21} cm^2). Moreover, by variation of the emission rate window, it is possible to measure the concentration profile of these oxide traps. The validity of the model and measurements are extensively discussed.

I. INTRODUCTION

Deep-level transient spectroscopy (DLTS) (Ref. 1) is a tool used to characterize insulator-semiconductor interfaces.[2–4] In metal-oxide-semiconductor (MOS) structures, the DLTS technique allows an estimate of the density of localized states at the oxide-semiconductor interface with better accuracy[5] than the capacitance voltage technique[6] or even than the conductance technique.[7] The technique basically consists of filling all the interface states during the pulse, then analyzing the emission rate during a temperature scan. In these conditions, the DLTS spectrum saturates when the pulse amplitude increases, because the interface states are completely filled. In the use of this saturating pulse DLTS (Ref. 2), we have observed in Si-SiO_2 MOS structures an unusual increase of the spectrum amplitude when the filling pulse amplitude or the pulse width increases, each independently of the other experimental parameters. The measurements are made on state-of-the-art MOS capacitors which exhibit a very low density of interface states ($N_{it} \approx 3 \times 10^9$ $cm^{-2} eV^{-1}$ at mid-gap).

We shall demonstrate here that this behavior can be understood by taking into account the possibility of tunneling between the oxide traps and the semiconductor. The DLTS technique allows a determination of the small concentration of these oxide traps ($N_{0t} \approx 10^7$–10^8 cm^{-2}). Moreover, by monitoring the DLTS signal amplitude versus the pulse width, it is also possible to measure the associated tunnel capture cross section ($\sigma_{nt} \approx 10^{-22}$–$10^{-21}$ cm^2) and determine the localization of these traps in the oxide ($\approx$10–30 Å from the interface). Presumably, the traps originate from the strained thin layer of the SiO_2 film near the interface.

In Sec. II, we show the experimental evidences of the tunneling effect. Section III gives the model and the calculation of DLTS response with tunneling. From these calculations we present, in Sec. IV, the procedure used to obtain the oxide traps characteristics. The results are given in Sec. V and discussed in Sec. VI.

II. EXPERIMENTAL EVIDENCES

The samples are made on a ⟨100⟩ oriented n-type 6–15 Ω cm Si substrate. The oxide, 1200 Å thick, is thermally grown at 950°C under wet atmosphere, followed by a N_2 annealing. The backside faces are degenerated by phosphorous implantation followed by annealing at 950°C for one hour in order to yield a perfect ohmic contact. Before DLTS measurements, $C(V)$ characteristics have been performed on each sample to verify their good electrical behavior and to determine the conditions of application of the DLTS technique.

The use of the saturating pulse DLTS requires two conditions. The pulse amplitude must bias the MOS capacitor in accumulation, so that all the interface states are below the Fermi level (Fig. 1). Second, the pulse width must be larger than the capture time constant, so all the interface states are filled at the end of the pulse. The capture time constant is given by

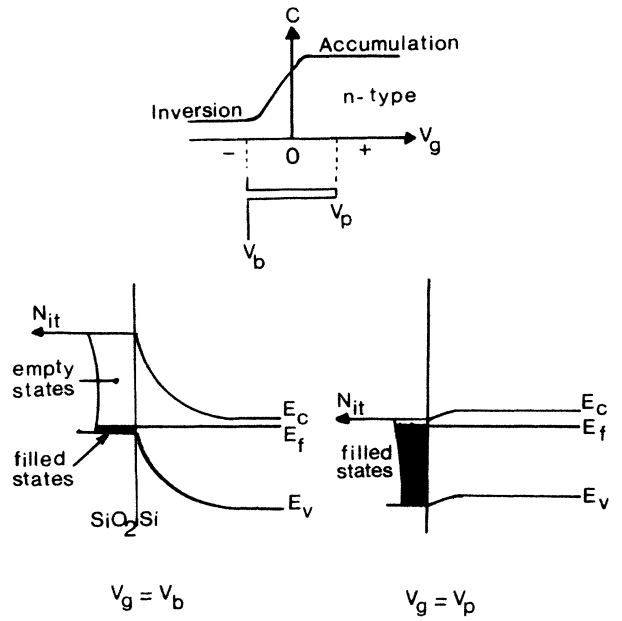

FIG. 1. Bias of a MOS structure during saturating pulse DLTS measurements and corresponding energy scheme.

$$\tau_c = (\sigma_n \bar{v}_n n_s)^{-1} , \quad (1)$$

where σ_n is the capture cross section of the interface states, $\bar{v}_n$ the average thermal velocity, and n_s the electron concentration at the interface. Typically, in weak accumulation (surface potential ψ_s about $5kT/e$) with σ_n about 10^{-18} cm^2 (the lowest reasonable value), the capture time constant varies from ≈ 3 μs at 70 K to 0.3 μs at 250 K. If these conditions are satisfied, the DLTS response saturates when the pulse amplitude and pulse width increase.

We have observed an unusual behavior of the samples described above. Figure 2 shows typical DLTS spectra obtained when the filling pulse voltage varies from 2.5 V to 8.5 V. The $C(V)$ characteristic, in the inset of Fig. 2, clearly reveals that the MOS structure is strongly in accumulation in this filling pulse range. Though the pulse width (chosen to be 20 μs) is larger than the capture time constant, the DLTS response does not saturate. The same behavior is observed when the filling pulse voltage is kept constant but when the pulse width varies. The amplitudes of the DLTS spectra, at various temperatures, as a function of the filling pulse voltage and of the pulse width are given in Figs. 3 and 4, respectively. Two kinds of behavior are shown in Fig. 3. Between 0 and a threshold value V_{p0}, the rapid variations of the DLTS signal are due to incomplete filling of the interface states. Above this threshold, we have not observed the usual saturating behavior (dotted line on Fig. 3) but a slow increase of the DLTS response. The role and the temperature dependence of the threshold value V_{p0} will be discussed later in Sec. IV. Figure 4 shows the behavior with the pulse width. As in Fig. 3, we observe an increase of the DLTS response instead of the expected saturating behavior. For

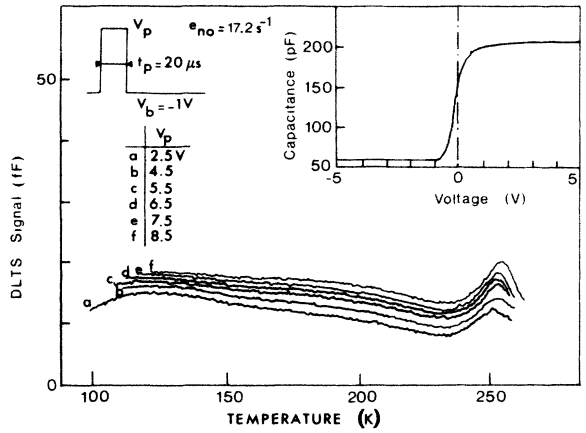

FIG. 2. Variation of the DLTS spectra vs the filling pulse amplitude V_P. The inset gives the $C(V)$ characteristic.

t_p smaller than 20 μs, we have not measured the filling kinetic of interface states. This limitation is due to our DLTS apparatus. Above 500 μs, the divergence is not significant because the ratio t_p/P of the pulse width over the period is in the range where the DLTS signal amplitude increases due to the behavior of our apparatus.[8] The pulse period is 0.1 s (i.e., the low frequency limit of our DLTS apparatus).

We shall explain such a behavior, by taking into account the effects of capture and emission of free carriers by defects in the oxide layer near the Si/SiO_2 interface and more precisely into the corresponding strained transition layer. These oxide traps are also historically called "slow interface states."[9] Section III is devoted to the tunneling model and the calculation of the modified DLTS response takes into account tunneling.

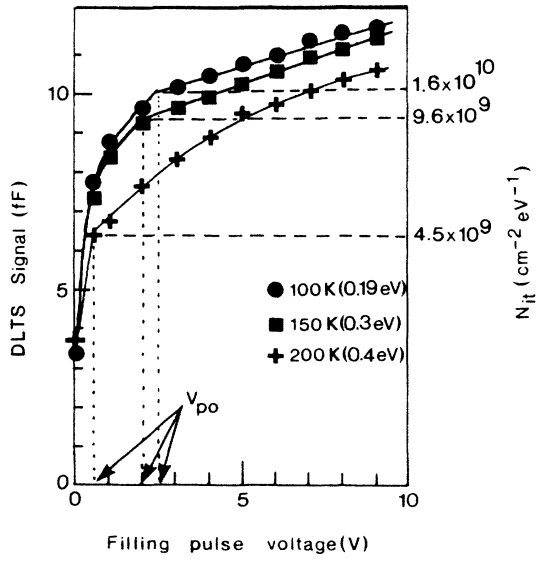

FIG. 3. Determination of the threshold-filling pulse voltage above which the oxide traps contribution is not negligible. Dotted lines correspond to the values without oxide traps, i.e., showing the saturation of interface states. The DLTS parameters are $V_b = -1$ V, $t_P = 20$ μs, and $P = 0.1$ s.

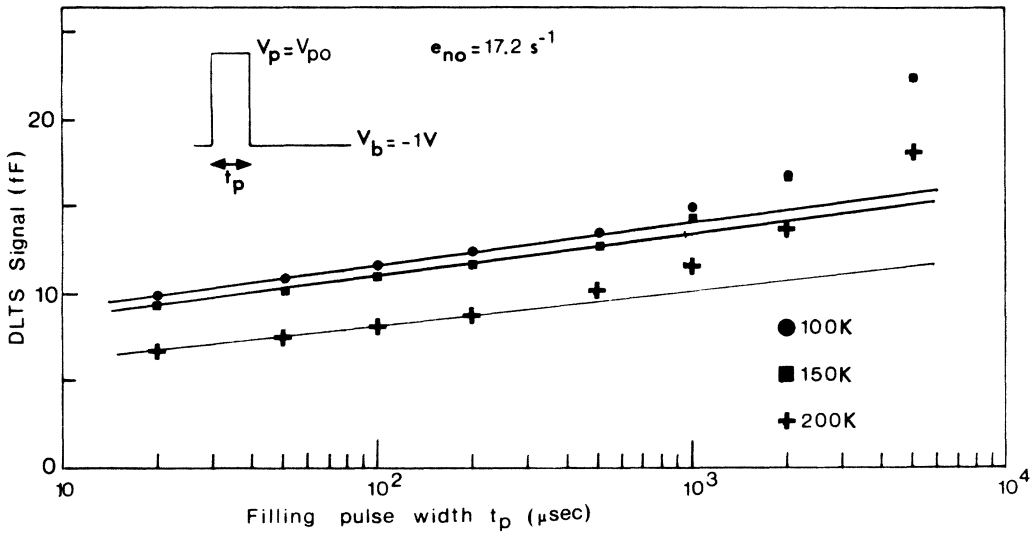

FIG. 4. Variations of the DLTS spectra amplitude vs the filling pulse width at various temperatures.

III. RESPONSE OF A MOS STRUCTURE WITH TUNNELING

In the saturating pulse DLTS, the transient capacitance in the temperature range where only the majority carriers dominate, is given by[10]

$$\Delta C(t) = A \int_{E_v}^{E_c} N_{it}(E) f(E,t) dE \ , \tag{2}$$

where $N_{it}(E)$ is the interface states density at an energy E between valence (E_v) and conduction (E_c) band extrema, $f(E,t)$ the majority carriers occupancy function, and t the time. The constant A is equal to

$$A = \frac{C^3}{\epsilon_s C_{ox} N_D} \ , \tag{3}$$

where C is the capacitance under bias voltage, ϵ_s the permitivity of Si, C_{ox} the oxide capacitance, and N_D the substrate doping concentration. Using an analysis of the transient by a double phases lock-in,[11] the DLTS response during a temperature scan is (see Appendix A)

$$R_{it}(T) = 0.48\ A\ N_{it}(E_w) kT \ , \tag{4}$$

where k is the Boltzmann's constant, T the absolute temperature, and E_w the location of the DLTS energy window in the band gap. This energy window, for which the interface traps respond within the lock-in period P at the temperature T, is given by

$$E_c - E_w = kT \ln \left[\frac{\sigma_n \bar{v}_n N_c}{e_{n0}} \right] \tag{5}$$

with the emission rate window e_{n0} equal to

$$e_{n0} = 1.72/P \ , \tag{6}$$

$\bar{v}_n$ and N_c are, respectively, the electron thermal velocity and the effective density of states in the conduction band. The capture cross section σ_n of the interface states must be known in order to deduce the spectroscopic information from the temperature scan. In the saturating pulse DLTS, the temperature shift of the DLTS spectra with the emission rate window does not allow a correct determination of σ_n because these measurements do not separate the temperature dependence from the energy dependence of the capture cross section.[12] Energy resolved DLTS should be applied to solve this problem,[13] but it was not used in this work because an accurate determination of the capture cross section of the interface states is not necessary in the study of the oxide traps. Consequently the correspondence between the temperature and the trap location in the Si band gap is usually made, assuming an average and constant capture cross section of 10^{-15} cm^2. This value is the mean value of the published results for about ten years.

We now introduce the possibility of electron tunneling between the oxide traps and the Si conduction band. We have chosen the simple case of tunneling through a trapezoidal barrier (Fig. 5). We have neglected the slope of the SiO$_2$ conduction band. This slope depends on the electric field across the oxide. In our case, the maximum applied field is 8×10^5 V/cm. The slope amplitude is $eFz \approx 80$ meV (with $z \approx 10$ Å) and this value is negligible compared to the barrier height. The emission rate associated with such a tunneling process from a level located at E_i below the SiO$_2$ conduction band (Fig. 5) to the substrate through a distance z is given by (see Appendix B)

$$e_t(E_i,z) = \alpha \exp \left[-2 \frac{(2m_1^* E_i)^{1/2}}{\hbar} z \right] \ , \tag{7}$$

where m_1^* is the SiO$_2$ electron effective mass, h the reduced Planck's constant. The exponential term corresponds to the tunneling through a square energy barrier with a height of E_i. The pre-exponential factor is (see Appendix B)

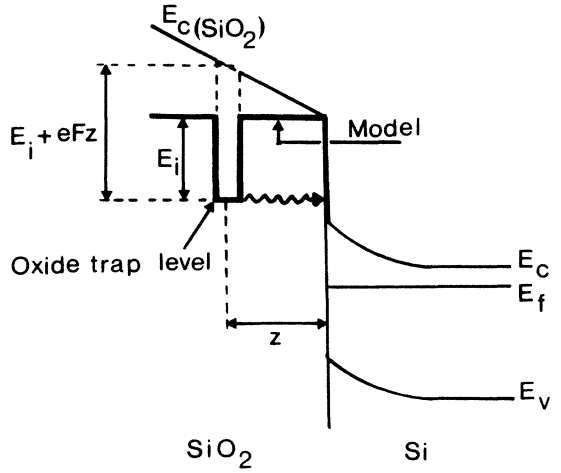

FIG. 5. Schematic representation of a tunneling effect through the the trapezoidal potential barrier of a Si-SiO_2 structure. The model used is a square barrier of height E_i.

$$\alpha=\frac{\hbar}{36m_3^*}\left[\frac{\pi}{2}\right]^5\frac{K_i^2}{K_i^2+k_i^2}\frac{k_1}{z}\ , \tag{8}$$

where m_3^* is the Si electron effective mass. The wave vectors K_i, k_i are defined in Appendix B.

Let us consider the simplest case of a single level E_i (Fig. 5) with a distributed concentration in the depth of the oxide N_{0t} (E_i,z). Because the filling pulse width is generally smaller than the capture time constant of oxide traps (see numerical values in Sec. V), they are not completely filled. We have a concentration n_{0t} (E_i,z) of trapped electrons during the pulse width, which are then re-emitted from these oxide traps. Assuming that the tunneling emission from oxide traps and the emission of the interface states are independent, the DLTS response becomes the sum of two contributions

$$R(T)=R_{it}(T)+A\int_0^\infty n_{0t}(E_i,z)\int_0^P \Gamma(T)\exp[-e_t(E_i,z)t]dt\,dz\ . \tag{9}$$

The first term is the contribution of interface states given by Eq. (4), and the other one is due to tunneling from the oxide trap, $\Gamma(t)$ being the correlation function of the double lock-in detector. Then, we obtain (see Appendix C)

$$R(T)=R_{it}(T)+0.723\ A\ n_{0t}(E_i,z_m)\ , \tag{10}$$

where z_m is the position of the maximum of the probe function (see Appendix C)

$$J(z)=\int_0^P \Gamma(t)\exp[-e_t(E_i,z)t]dt \tag{11}$$

and is related to the lock-in emission rate window e_{n0} by

$$z_m=\frac{\hbar}{2(2m_1^*E_i)^{1/2}}\ln\left[\frac{\alpha}{e_{n0}}\right]\ . \tag{12}$$

Thus, if we consider oxide traps located at a single energy level E_i, the tunneling emission induces a shift of the DLTS spectrum independent of the temperature (if the term A is independent of the temperature, see below in Sec. V). From this shift we can deduce the concentration of electrons trapped on the oxide traps $n_{0t}(E_i,z_m)$ and, if E_i is known, the depth z_m where the contribution of these traps is maximum. Varying the emission rate window e_{n0} allows, in principle, the determination of the concentration profile. The assumption of a single energy level will be discussed in the next section.

This model will be used in the following to calculate the DLTS response with tunneling from oxide traps. The limitations will be discussed in Sec. VI. From these calculations, we present in the following sections (i) the procedure used to obtain the oxide traps characteristics (Sec. IV), and (ii) the experimental results (Sec. V).

IV. DATA ANALYSES PROCEDURE

We obtain the concentration of electrons trapped on oxide traps $n_{0t}(E_i,z_m)$ from Eq. (10). For that, it is necessary to know the interface states contribution $R_{it}(T)$. That is done from the experimental results of Fig. 3. As explained in Sec. II, the threshold value V_{p0} of the filling pulse amplitude separates two kinds of behaviors. Consequently, it is reasonable to consider the DLTS response at $V_p=V_{p0}$ as due to the interface states only. Indeed, all the interface states are filled and the contribution of oxide traps is negligible. These conditions minimize the oxide traps response but also allow a correct determination of the interface states density. The values of N_{it} are given in Fig. 3. We also give the energy of the interface states analyzed by the DLTS measurements [Eq. (5)]. This allows us to explain the variations of the threshold value V_{p0}. According to Eq. (5), the interface traps near the conduction band (which respond at low temperature) require the largest band bending variation to be completely filled, and consequently the largest threshold filling pulse amplitude.

Normally the same procedure should be used to choose the optimal pulse width in order to determine the interface states contribution. From Fig. 4, we cannot see a threshold value of the pulse width. So we have chosen the smallest pulse with ($t_p=20$ μs) as the reference value to measure the interface states contribution. This leads to an error in the determination of the trapped electrons concentration n_{0t} (E_i,z) which will be discussed in Sec. V. As a consequence, we take the interface states density determined above from Fig. 3 as the "reference values" to estimate $R_{it}(T)$ in Eq. (10) using Eq. (4).

The last point concerning the measurement parameters is the choice of the bias voltage V_b. The value of bias voltage V_b is chosen at the boundary between weak and strong inversion. With this condition, the minority carriers response[14] and the cutoff effect[12] occur above 260 K, and the DLTS measurements will be valid. From the $C(V)$ characteristic (inset of Fig. 2) we deduce $V_b=-1$ V.

After the preliminary determination of the interface states contribution we obtain, from the experimental results of Fig. 4, the filling kinetics of the oxide traps, i.e.,

the curve $n_{0t}(E_i,z)$ versus t_p. We assume that all the electrons trapped on oxide traps during the pulse width t_p are re-emitted during the transient regime. This assumption is valid when the period of the pulse P is larger than the time constant of the emission e_t^{-1}. From Appendix C, we see that a limitation occurs for $z=z_m$ where $e_t(z_m)=e_{n0}=1.72/P$. Indeed, from Eq. (7) giving the variations of the tunneling emission rate, it can be seen that the assumption remains valid for all the traps located between the interface and the depth z_m given by Eq. (12). With this assumption, the measured concentration $n_{0t}(E,z)$ is, in fact, the concentration of trapped electrons (or a partial concentration if the previous assumption is not valid). From the filling kinetics, we can deduce the oxide traps concentration N_{0t} and the capture time constant (τ) of these oxide traps. Indeed, if the behavior of the filling kinetics follows the classical kinetic rate equation, we have

$$n_{0t}=N_{0t}[1-\exp(-t_p/\tau)] . \tag{13}$$

The capture occurs when the MOS structure is biased in accumulation and the corresponding electron density at the interface is

$$n_s=N_D \exp\left[\frac{e\psi_s}{kT}\right] , \tag{14}$$

where N_D is the doping concentration. The ratio $e\psi_s/kT$ of the surface potential over the thermal energy unit kT/e is measured at various temperatures by the $C(V)$ analysis. This ratio is found fairly constant for a given filling pulse V_p and for any temperature. Then, to define an associated tunneling capture cross section σ_{nt}, we use the well-known classical expression of a capture time constant

$$\tau=(\sigma_{nt}\bar{v}_n n_s)^{-1} , \tag{15}$$

where the electron thermal velocity $\bar{v}_n$ of SiO_2 is obtained with an effective mass of 0.64 m_0, with m_0 the electron mass.[15] Then the fit of Eqs. (13) to (15) with the experimental kinetics allows the determination of N_{0t} and σ_{nt}. The experimental results are given in the next section.

Finally, how we can deduce the energy and depth localization of the oxide traps? This localization is given by the maximum of the probe function $J(z)$ [Eq. (11)]. The maximum occurs when the tunneling emission is equal to the emission rate window of the DLTS apparatus (see Appendix C). Thus we obtain the locus of oxide traps for which $\sqrt{E_i}z_m$ is constant. The deconvolution between energy and depth is not obvious and in order to have a numerical value of z_m, we have assumed a single value of E_i. Then, the depth localization will be evaluated by Eq. (12). We have chosen several values of E_i between the SiO_2 conduction band and the limit $E_i=3.25$ eV, i.e., the validity range of our model (see Sec. VI). The value of 3.25 eV is the barrier height from the Si and SiO_2 conduction bands. It has been measured by electron photoinjection and photoemission.[16] The simplifying assumption of a single energy level arises from the will to obtain an easy numerical evaluation of the tunneling effect. It is probably not an accurate physical description of the strained transition layer. Improvements of this model will be proposed in Sec. VI. Following the procedure described above, we present the experimental results in the next section.

V. EXPERIMENTAL RESULTS

The filling kinetics are given in Fig. 6. The full lines are the best fits of Eq. (13) obtained by the least-squares method. The two fit parameters are N_{0t} and σ_{nt}. Table I summarizes the results of the fits. The temperature variations shown on Fig. 6 are not significant because they are smaller than the experimental error bars. These error bars are deduced from the experimental errors on the DLTS spectra amplitudes ($\Delta R/R \approx 0.01$–0.03 with our apparatus), from the uncertainty in the capacitance measurements ($\Delta C/C=0.02$ with our capacitance meter) and from the uncertainty on the doping concentration ($\Delta N/N=0.05$) deduced from the $C(V)$ analysis. The result is about $\Delta N_{0t}/N_{0t} \approx 0.2$ to 0.5. Moreover we have shown in Sec. IV that the choice of $t_p=20$ μs for the determination of the interface states contribution probably induces an error in the filling kinetics but this error is negligible compared to the previous ones. Thus, we consider only a mean value for N_{0t} and σ_{nt}. They are, respectively, $N_{0t}=3.5\times10^7$ cm^{-2} for the oxide traps concentration and $\sigma_{nt}=5.6\times10^{-22}$ cm^2 for the associated tunneling capture cross section.

In order to validate our previous model [Eq. (10)] the difference between the spectrum amplitude $R(T)$ and the interface states contribution $R_{it}(T)$, i.e., the oxide traps contribution, must be temperature independent. From Eq. (10), this difference is temperature independent only if it is also the case for the term A. With conventional DLTS, the base line capacitance C varies slowly with the temperature, as a consequence of the variation of the metal semiconductor work-function difference, so the term A is slowly varying [see Eq. (3)]. To overcome this problem, without the use of constant capacitance DLTS, we have directly calculated the concentration of trapped electrons from the data of Fig. 2. The variations of this measured

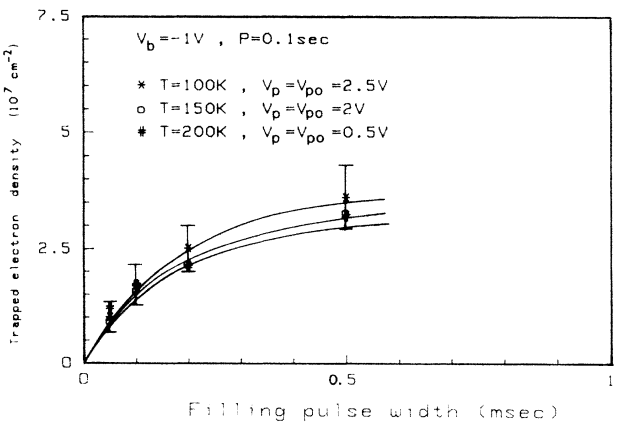

FIG. 6. Filling kinetics of the oxide traps deduced from the data of Fig. 4. The error bars are given for $T=100$ K. The full lines are the best fits of Eq. (13).

TABLE I. Concentration, time constant, and associated tunneling capture cross section of the oxide traps obtained by fitting the experimental kinetics with Eq. (13).

T (K)	N_{0t} (cm^{-2})	τ (μs)	σ_{nt} (cm^2)
100	$3.83\ 10^7$	179	$6.6\ 10^{-22}$
150	$3.52\ 10^7$	183	$5.5\ 10^{-22}$
200	$3.3\ 10^7$	180	$4.6\ 10^{-22}$
Mean value	$3.5\ 10^7$	181	$5.6\ 10^{-22}$

concentration versus temperature are given in Fig. 7 for different filling pulse amplitudes. Taking into account the error bars, the temperature independence seems to be verified. A more accurate discussion will be given in Sec. VI.

Following the procedure given in Sec. IV, we have estimated the depth localization of the oxide traps characterized by the filling kinetics of Fig. 6 with several values of E_i. The pre-exponential factor of the tunneling emission rate [Eq. (8)] is about $10^{13}\ s^{-1}$. From Eq. (12) we obtain the values reported in Table II. In order to obtain the profile of these oxide traps, Fig. 8 shows the variation of the DLTS spectrum amplitude at a given temperature when the emission rate window e_{n0} varies. According to

TABLE II. Depth localization in the oxide for different deep trap levels.

E_i (eV)	$\sqrt{E_i} z_m$	z_m (Å)
2	36.6	26
3	35.3	20.4
3.2	32.7	18.3

Eq. (12) we expect to obtain the oxide traps profile. Such a variation of the amplitude cannot be explained by the increase of the DLTS response when the ratio t_p/P increases[8] because this ratio is kept smaller than 10^{-2} s with $t_p = 20\ \mu s$. The validity of the profile measurements will be discussed in the next section.

VI. DISCUSSION

The oxide traps filling kinetics are fitted by the classical kinetic equation. These filling kinetics explain easily the unusual variations of the DLTS spectra with the pulse width. Moreover, they also explain the variations with the pulse amplitude (Figs. 2 and 3). Indeed, this effect is not taken into account, in our model, by a field-enhanced tunnel emission (Poole-Frenkel effect). From Eqs. (13)–(15) it is obvious that the filling kinetics are dependent on the filling pulse amplitude. This modulation occurs by the modulation of the carriers density n_s at the interface. Figure 9 shows the theoretical behavior of Eq.

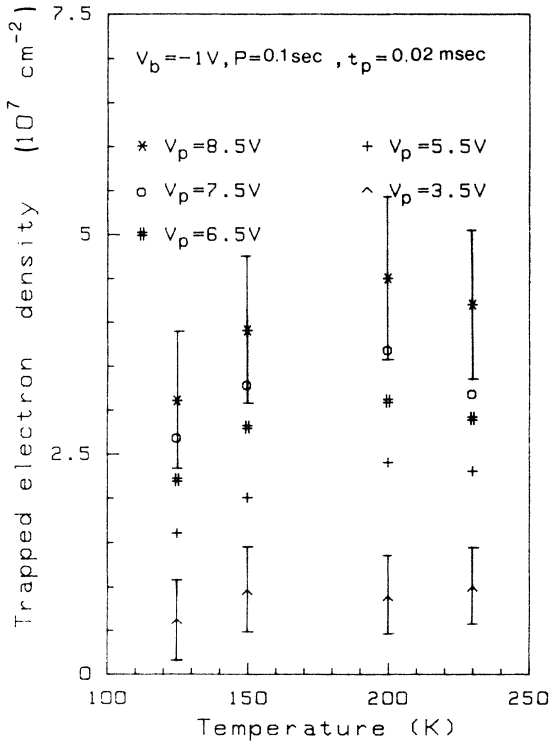

FIG. 7. Variations of the trapped electron density vs the temperature for different filling pulse amplitudes deduced from the data of Fig. 2. The error bars are given for $V_P = 3.5$ V and $V_P = 8.5$ V.

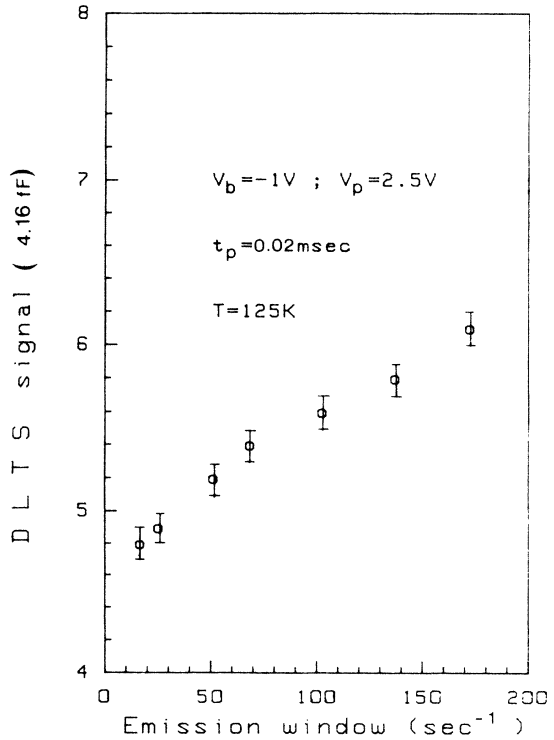

FIG. 8. Behavior of the DLTS response when the emission rate window varies.

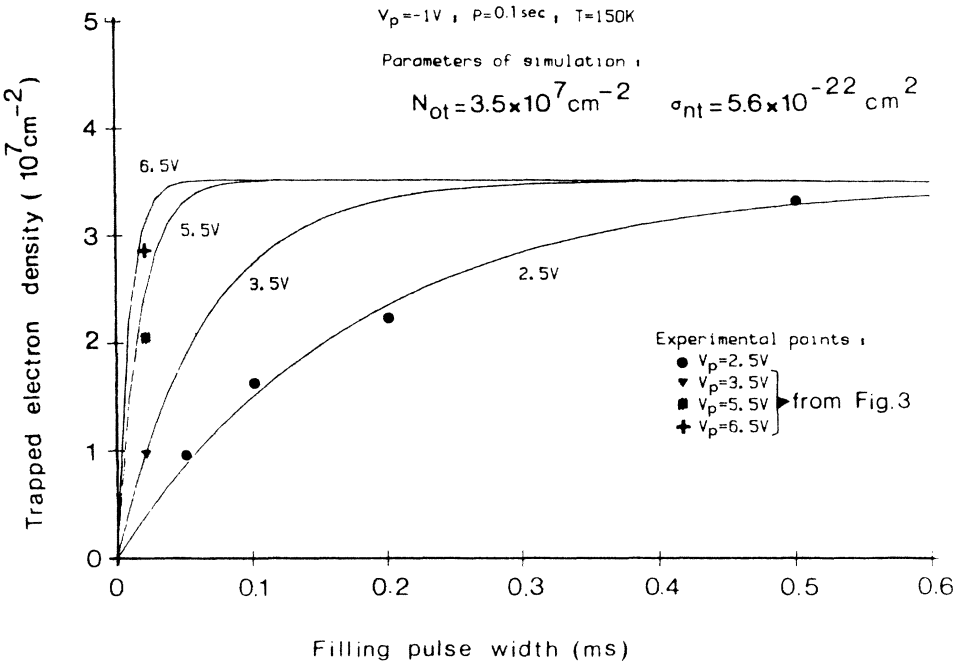

FIG. 9. Comparison between the experimental data obtained for various filling pulse amplitudes and a simulation of the filling kinetics given by Eq. (13).

(13) calculated with the values of N_{0t} and σ_{nt} given in Sec. V, and at $T=150$ K. The data of Fig. 3 (obtained with $t_p=20$ μs), reported on Fig. 9, clearly explain the evolution of the measured values n_{0t} versus the filling pulse amplitude. In order to improve this experimental verification, the study of the complete filling kinetics with the other values of V_p is under investigation.

The same way can be used to explain the experimental results given in Fig. 7. As explained in Sec. V, we now try to see if the tunnel emission is temperature dependent or not, in order to validate our model. The observation of the oxide traps filling kinetics (Fig. 6) seems to lead to the validation of a temperature-independent tunneling phenomenon (not phonon assisted) as we have assumed in Sec. III. From Fig. 7, the temperature independence seems to be verified (taking into account the error bars), but a small increase with the temperature is still possible. The data of Fig. 7, measured with a pulse width $t_p=20$ μs, are very sensitive to the change of the capture time constant (τ) of the oxide traps because t_p is smaller than τ. When the temperature increases, it is obvious from Eq. (15) that the tunneling capture time constant decreases. If we assume that the associated tunneling capture cross section is temperature independent, this variation is only due to the dependence of the thermal velocity $\bar{v}_n$. Thus, we have the same kind of behavior as for n_{0t} vs V_p. At a given pulse width, smaller than the capture time constant, the measured value of n_{0t} must increase with the temperature. Figure 10 shows the comparison between the experimental results and a simulation performed using, as parameters, the mean values of N_{0t} and σ_{nt} deduced previously. The agreement is good; this seems to prove the validity of an independent temperature tunneling emission. The low temperature variations are only due to the temperature dependence of the electron thermal velocity.

The conclusion of the above discussion is that in the tunnel emission from oxide traps we can neglect the phonon-assisted effect and the electric field enhancement (Poole-Frenkel effect).

We now discuss the validity of the profile measurements. From Fig. 8 and Eq. (10), the variation of the trapped electron density Δn_{0t} is equal to 4×10^{7} cm^{-2}. The corresponding depth variation is given by Eq. (12); we have $\Delta z_m=1.6$ Å. The slope of the profile is 2.5×10^{-7} cm^{-2} Å^{-1}, a reasonable value. For example, taking the

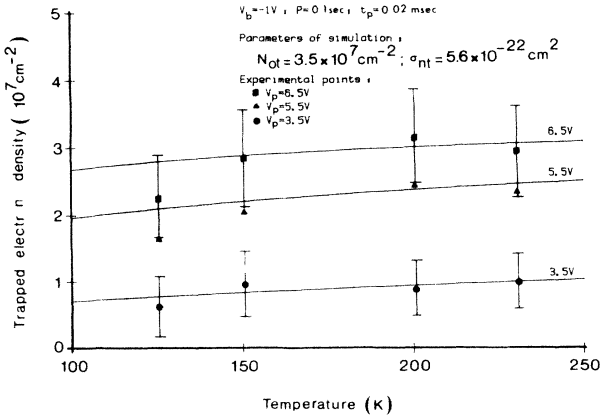

FIG. 10. Comparison between the theoretical temperature dependence of the trapped electron density [given by Eq. (13)] and the experimental measurements.

interface states density at $z=0$ ($N_{it}=5\times10^{9}$ cm^{-2} eV^{-1}) and two other values of the trapped electron density deduced from Fig. 8 for ($e_{n0}=17.2$ and 172 s^{-1}), the fit of an assumed exponential depth variation shows that the density of oxide traps vanish at $z\approx30$ Å. This value, which can be regarded as the strained layer depth of SiO_2, is a good size order.[17] If the oxide trap profile seems to be possible, two limitations occur. First, we can observe only a small region, due to the frequency limitation of the DLTS measurements (typically $P=0.1$–0.01 s). Second, we cannot deduce directly the oxide traps concentration profile from a simple curve, such as the one given by Fig. 8, because we have not the oxide traps concentration N_{0t} but the trapped electron density n_{0t} at a given pulse width (here $t_p=20$ μs). We need complete filling kinetics (as given in Fig. 6) at various emission rate windows.

In view of all these results, several remarks are necessary. For a depth about 30 Å the highly disordered atomic structure should be evident on such a scale. Consequently, from a theoretical standpoint, the model used above must be regarded as too primitive. A more elaborate model must take into account a spatial and energy distribution of the traps in the oxide layer and in the silicon band-gap, respectively. Such a model has been introduced by Hasegawa and Sawada.[18] Meanwhile, their model is not useful in our case. Several points must be improved. The distinction between the interface states density N_{it} and the oxide traps concentration is not allowed because they use a fictitious density:

$$N=\int_0^{z_m} N_T(E,z)dz\ , \tag{16}$$

where $N_T(E,z)$ is the spatial and energy distribution of the traps, and z_m the maximum depth explored in the oxide at given experimental parameters. Moreover, their model is developed for the case of weak-amplitude filling pulses. A more elaborate model would include a distinction between two energy regions. For oxide traps located between the SiO_2 conduction band and the Si conduction band (i.e., $E_i<3.25$ eV in Fig. 5) our previous model remains valid. But, for $E_i>3.25$ eV, it would include a cascade emission through the interface states. The first phenomena is a tunnel emission through the square barrier height from the oxide traps to interface states. The second is the thermal emission from interface states to the Si conduction band. In this case, the DLTS time constant window e_{n0} allows us to select the locus of $\sqrt{E}.z$ for the tunnel emission and the energy value for the thermal emission. Thus, the energy and depth location of oxide traps would be possible. This model is under study.

Another question is related to the observation of such a tunneling effect using the classical conductance measurements. Attempts were made by Heiman and Warfield[9] and later by Preir[19] to explain the frequency dispersion in conductance measurements by a tunneling effect, but these attempts were not successful. However, tunneling effects were detected in case of large oxide traps concentration ($\approx10^{10}$–10^{11} cm^{-2}) produced by electron irradiations[20] or for amorphous carbon on silicon structures.[21] In our state-of-the-art metal-oxide-silicon structures we have been unable to detect any tunneling effect by the conductance technique. This fact is an additional illustration of the sensitivity of the DLTS technique over the conductance technique for the characterization of insulator-semiconductor interfaces.

Finally, a similar tunneling effect is not observed on p-type MOS capacitors. A reasonable explanation for this, as well as for the carriers injection phenomena[22] from the silicon substrate into SiO_2 is the larger energy barrier that holes have to overcome, as compared to electrons, to be injected into silicon.

The low density of oxide traps obtained by this analysis naturally raises questions regarding possible artifactual or alternative physical origins of this unusual behavior of the DLTS response. For example, could MOS capacitor edge effects (i.e., fringing fields) play any role? It is not the case because such effects are independent of the substrate (n or p type) and we have observed a crucial dependence as explained above. In fact, the exact nature of the Si-SiO_2 interface is not yet fully understood. An appealing picture from XPS results[23] suggests a stoichiometric strained layer that extends to 20 at 40 Å into the oxide. This should be considered as a substantiated basis for a defect model. In our samples the total oxide charge, including mobile ionic charges, oxide trapped charges, and fixed oxide charges, deduced from the flat-band voltage on the $C(V)$ curve (see Fig. 2), is $3.6\times10^{+10}$ cm^{-2}. This value is a good and classical low density, essentially due to ionic and oxide trapped charges, but it is not possible to know, from the flat-band voltage, the exact contribution of the fixed oxide charges in the strained layer. So, there is not an obvious correlation between the oxide traps that we have observed by DLTS and the fixed oxide charges, hence the physical origins cannot be better understood at this stage.

VII. CONCLUSIONS

We have used the DLTS technique to characterize the oxide traps in SiO_2 film which interact with the silicon substrate by tunneling in state-of-the-art MOS structures. Incorporating a simple model of this effect in the derivation of the DLTS signal, we have been able to obtain the filling kinetics of these traps; we have deduced their concentration which, in the case of the structures under study, is 10^{7}–10^{8} cm^{-2}, their associated tunneling capture cross section ($\approx10^{-22}$–10^{-21} cm^2), and their localization. These traps are located at 10 to 30 Å from the interface, i.e., in the strained layer of the SiO_2 film. We have shown that the tunneling emission is not phonon assisted and not electric field enhanced. Further measurements and models are under study in order to improve the DLTS characterization of the first layers of the SiO_2 film.

ACKNOWLEDGMENTS

The authors are indebted to E. Rosencher (Centre National d'Etudes des Télécommunications, Meylan, France) for helpful discussions and for providing the samples used in this study. This work was supported under GCIS (Groupement Circuit Intégré Silicium) contract. The Laboratoire de Physique des Solides is "Laboratoire No. 253

associé au Centre National de la Recherche Scientifique." The Groupe de Physique des Solides de l'Ecole Normale Supérieure is "Laboratoire No. 17 associé au Centre National de la Recherche Scientifique."

APPENDIX A

In this appendix, we establish the theoretical expression of the amplitude $R(T)$ of the DLTS spectrum for an interface state distribution in the case of a double phase lock-in analysis. The response of a lock-in detector to a transient signal $\Delta C(t)$ is

$$R(T)=\int_0^P \Gamma(t)\Delta C(t)dt \ , \tag{A1}$$

where $\Delta C(t)$ is given by Eq. (1) in the text and $\Gamma(t)$ is the correlation function of the double lock-in detector. P is the period of the transient signal. The $\Gamma(t)$ function is defined by

$$\Gamma(t)=\begin{cases} 0 \ \text{for} \ 0<t<P/4 \ , \\ \pi/\sqrt{2}P \ \text{for} \ P/4<t<P/2 \ , \\ 0 \ \text{for} \ P/2<t<3P/4 \ , \\ -\pi/\sqrt{2}P \ \text{for} \ 3P/4<t<P \ . \end{cases} \tag{A2}$$

Thus we must calculate the following integral:

$$R(T)=A\int_0^P \Gamma(t)\int_{E_v}^{E_c} N_{it}(E)f(E,t)dE\,dt \ , \tag{A3}$$

where the constant A is defined in the text. The occupancy function of a level at an energy E below the conduction band is[10]

$$f(E,t)=\exp[-e_n(E)t] \ . \tag{A4}$$

The emission rate is well known:

$$e_n(E)=e_n^* \exp\left[\frac{E_c-E}{kT}\right] \tag{A5}$$

with the pre-exponential factor $e_n^*=\sigma_n\bar{v}_nN_c$. Then Eq. (A3) is rewritten

$$R(T)=\frac{\pi A}{\sqrt{2}P}\int_{P/4}^{P/2}\int_{E_v}^{E_c} N_{it}(E)\left\{\exp(-e_nt)-\exp\left[-e_n\left[t+\frac{P}{2}\right]\right]\right\}dE\,dt \ , \tag{A6}$$

where the integral over the time period $(3P/4,P)$ is easily reduced to $(P/4,P/2)$. Inverting (A5) we can rewrite

$$R(T)=\frac{\pi AkT}{\sqrt{2}P}\int_{P/4}^{P/2}\int_{e_n(E_v)}^{e_n(E_c)} N_{it}(E)\left\{\exp(-e_nt)-\exp\left[-e_n\left[t+\frac{P}{2}\right]\right]\right\}\frac{de_n}{e_n}dt \ . \tag{A7}$$

Because the integrand is a narrow peaked function the bounds in the integral can be taken from $e_n=0$ to $e_n=\infty$, and since we assume that $N_{it}(E)$ is slowly varying over the integrand, we obtain

$$R(T)=\frac{\pi AkT}{\sqrt{2}P}N_{it}(E_w)\int_{P/4}^{P/2}\int_0^{\infty}\left\{\exp(-e_nt)-\exp\left[-e_n\left[t+\frac{P}{2}\right]\right]\right\}\frac{de_n}{e_n}dt \ , \tag{A8}$$

where E_w is the energy position of the maximum of the peak, given by $e_n(E_w)=e_{n0}$, i.e., by Eq. (5) in the text. The results is[24]

$$R(t)=\frac{\pi AkT}{\sqrt{2}P}N_{it}(E_w)\int_{P/4}^{P/2}\ln\left[\frac{t+P/2}{t}\right]dt \ , \tag{A9}$$

and the integral is easily obtained:

$$R(T)=\frac{\pi AN_{it}(E_w)kT}{\sqrt{2}P}\left[t\ln\left[\frac{t+P/2}{t}\right]+\frac{P}{2}\ln\left[t+\frac{P}{2}\right]\right]_{P/4}^{P/2} \ . \tag{A10}$$

Finally, we obtained the following result:

$$R(t)=0.48 \ \text{A} \ N_{it}(E_w)kT \ . \tag{A11}$$

We now derive the expression of the energy window, i.e., the energy localization of the traps which contribute to the DLTS response $R(T)$ at a given temperature. For this, Eq. (A3) is rewritten

$$R(T)=A\int_{E_v}^{E_c} N_{it}(E)J(E)dE \tag{A12}$$

with

$$J(E)=\int_0^P \Gamma(t)f(E,t)dt \ . \tag{A13}$$

The calculation of $J(E)$ is obvious and we obtain

$$J(E)=\frac{\pi}{\sqrt{2}Pe_n}\left[\exp(-e_nP)-\exp\left[-\frac{3e_nP}{4}\right]-\exp\left[-\frac{e_nP}{2}\right]+\exp\left[-\frac{e_np}{4}\right]\right] \ . \tag{A14}$$

This function is the energy window and a computer simulation is given in Fig. 11 at 77 and 250 K. The maximum of $J(E)$ occurs at the energy E_w given in the text by Eqs. (5) and (6). The solution of Eq. (6) is not analytical but is derived from a computer simulation. We have also verified the validity of the analytical solution of the DLTS

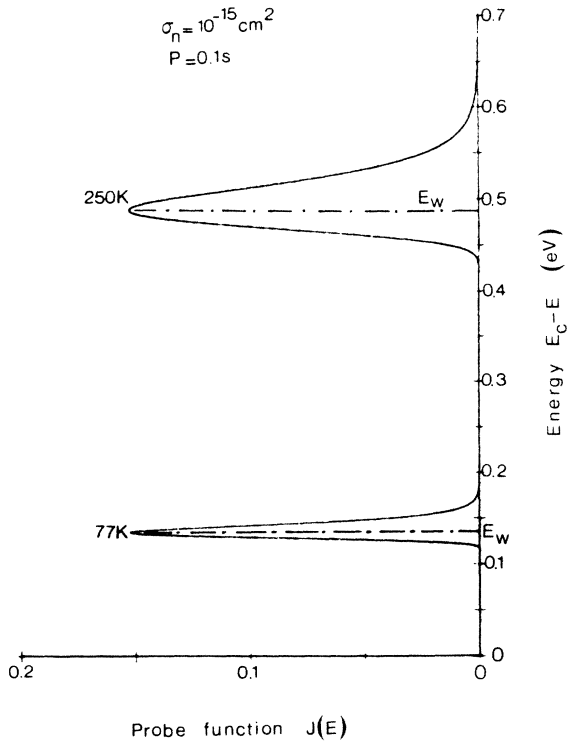

FIG. 11. The energy window given by Eq. (5) and Eq. (A14) in the case of a double lock-in analysis.

response given by Eq. (A11). Substituting Eq. (A14) for $J(E)$ into Eq. (A12) and using a computer integration with the trapezoidal rule, we have obtained the same results with Eq. (A11). Finally, the energy resolution of the DLTS method is given by the half-height width of the energy window function $J(E)$. From Fig. 11 we obtain 17 meV at 77 K and 55 meV at 250 K. Note that these calculations are valid in the range $t_p/P < 10^{-2}$ s, where the influence of the pulse width is negligible.[8]

APPENDIX B

In this appendix we evaluate the transition probability from oxide traps to the substrate. It is well known that this probability must decrease exponentially with z, the distance between the oxide trap and the interface, but at least the pre-exponential factor is not well defined. We develop here a simple model using the effective mass approximation to calculate the tunneling transition probability from an initial state $|i\rangle$ (energy E_i) eigenstate of a spherical square-well potential of depth V_0 to a continuum of free state $|f\rangle$ in the substrate conduction band. Figure 12 gives the energy diagram along the z direction.

The initial wave function $|\psi_i\rangle$ is easily obtained by assuming a spherical symmetrical state (s state) of the electron in the square well. The radial solution of the Schrödinger's equation inside the well of width a is

$$\psi_i(r)=\left[\frac{K_i}{2\pi(1+K_i a)}\right]^{1/2}\sin(k_{i1}r) \tag{B1}$$

and the wave numbers are given by

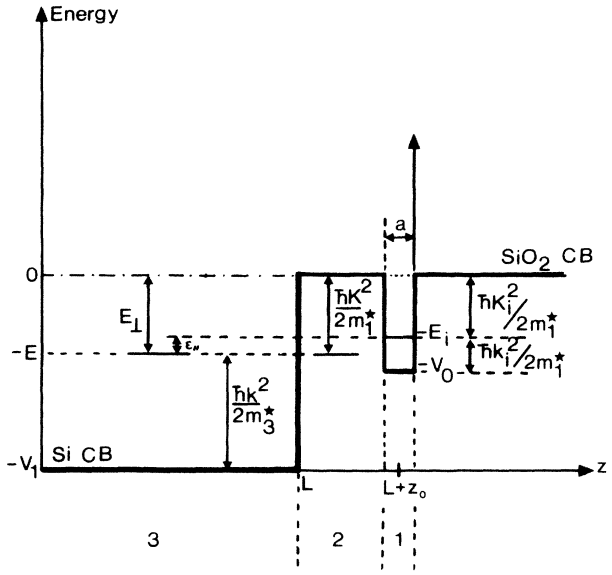

FIG. 12. Energy diagram used in the calculation of the tunneling transition probability.

$$k_{i1}^2=\frac{2m_1^*}{\hbar}(V_0-E_i) \text{ in region 1 ,} \tag{B2a}$$

$$K_i^2=\frac{2m_1^*}{\hbar}E_i \text{ in region 2 ,} \tag{B2b}$$

where m_1^* is the effective mass of electron in the SiO_2.

The same method is used to treat the Si-SiO_2 interface. The one-dimensional problem is exactly the same, but now the semiconductor thickness L is greater than a. At zero, we have taken an infinite barrier height to quantify the continuum of states at the backside of the Si substrate. Along the z direction, the solutions of the Schrödinger equations are

$$\psi_2(z)=\left[\frac{1}{2\pi L}\right]^{1/2}\left[\pm\frac{k}{K'}\right]\frac{m_1^*}{m_3^*}\exp[-K(z-L)] \tag{B3}$$

in region 2, and

$$\psi_3(z)=\left[\frac{1}{2\pi L}\right]^{1/2}\sin kz \tag{B4}$$

in region 3 (Si substrate). Let us consider an electron at energy E, we have

$$K^2=\frac{2m_1^*}{\hbar}E \text{ in region 2 ,} \tag{B5a}$$

$$k^2=\frac{2m_3^*}{\hbar}(V_1-E) \text{ in region 3 ,} \tag{B5b}$$

where m_3^* is the electron effective mass in the Si and in the z coordinate, V_1 is the barrier height between the conduction band of Si and SiO_2. In Eq. (B3) we define $K'^2=k^2+K^2$. The normalization constants of ψ_2 and ψ_3 are obtained using the approximation $KL \gg 1$ and assuming a continuity condition of the wave functions at the interface ($z=L$) and of the terms $1/m^*\delta/\delta z$ of these wave functions.

From the Oppenheimer approach,[25] the transition prob-

ability per unit time is

$$W=\frac{2\pi}{\hbar}\sum_f |\langle\psi_i|V_f|\psi_f\rangle|^2\delta(E_i-E_f)\ . \tag{B6}$$

The above result can be transformed to a more convenient form. Writing $V_f=V_i+H_i-H_f$ where V_f, V_i are, respectively, the final and initial potentials and H_f and H_i are the Hamiltonians in the final and initial states, we obtain

$$W=\frac{2\pi}{\hbar}\sum_f |\langle\psi_i|V_i|\psi_f\rangle+(E_f-E_i)\langle\psi_i|\psi_f\rangle|^2 \times\delta(E_i-E_f) \tag{B7}$$

i.e.,

$$W=\frac{2\pi}{\hbar}\sum_f |\langle\psi_i|V_i|\psi_f\rangle|^2\delta(E_i-E_f)\ , \tag{B8}$$

where $V_i=-V_0$ is the potential barrier corresponding to the initial state. The initial wave function is given by Eq. (B1) and the final wave function is obtained, with this formalism, from the wave function in the region 2 given by Eq. (B3). The final free-electron wave function in this case is

$$\psi_f=\psi_2(z)\frac{\exp(i\mathbf{k}_{||}\cdot\mathbf{r}_{||})}{\sqrt{S}} \tag{B9}$$

assuming a Bloch's wave propagation in x and y coordinates. S is the area of the Si-SiO$_2$ interface. Thus, we can rewrite the matrix $M_{if}=\langle\psi_i|V_i|\psi_f\rangle$

$$M_{if}=-V_0\int_0^a r\sin k_{i\,1}r\int_{\theta,\Phi}\sin\theta\,d\theta\,d\Phi\left[\frac{K_i}{2\pi(1+K_ia)}\right]^{1/2}\frac{\exp(i\mathbf{k}_{||}\cdot\mathbf{r}_{||})}{\sqrt{S}}\left[\frac{1}{2\pi L}\right]^{1/2}\left[\pm\frac{k}{K'}\right]\frac{m_1^*}{m_3^*}\exp[-K(z-L)]\ . \tag{B10}$$

Such a triple integral is easier to evaluate in the limit of an initial Dirac one-dimensional potential well, i.e., $K_ia\to 0$. In this case we must have

$$V_0a^2\to\frac{\hbar^2}{2m_1^*}\left[\frac{\pi}{2}\right]^2\ , \tag{B11a}$$

$$k_{i\,1}a\to\frac{\pi}{2}\ . \tag{B11b}$$

After elementary calculations, including these results, the matrix element reduces to

$$M_{if}=\pm\frac{\hbar^2}{3m_3^*}\left[\frac{\pi}{2}\right]^3\frac{\sqrt{K_i}k}{K'\sqrt{V}}\exp(-Kz_0)\ , \tag{B12}$$

where V is the silicon volume. Then, the summation over the final states is transformed into a triple integral in k space. The energy of final states is $E_f=E_\perp-\epsilon_{||}$ with $E_\perp=-E$ to respect the notation of Fig. 12 and Eq. (B5). Using the densities of states

$$n(E_\perp)=\frac{L}{\pi}\frac{m_3^*}{\hbar^2k^2}\ , \tag{B13a}$$

$$n(\epsilon_{||})=\frac{m_3^*S}{2\pi\hbar^2}\ , \tag{B13b}$$

we perform the integration on the energies and obtain

$$W=\frac{1}{18\hbar}\left[\frac{\pi}{2}\right]^5\frac{K_i}{K'^2}\int_{-V_1}^{\infty}k\exp(-2Kz_0)dE \times\int_0^{\infty}\delta(E_i-E_\perp-\epsilon_{||})d\epsilon_{||}\ . \tag{B14}$$

The integral over $E_\perp$ is reduced from V_1 to $-E_i$ (see Fig. 12), and taking into account the δ function the integral over $\epsilon_{||}$ is reduced to unity. Using a variable change from Eq. (B5), we rewrite

$$W=\frac{\hbar}{18m_3^*}\left[\frac{\pi}{2}\right]^5\frac{K_i}{K'^2}\int_0^{k_i}k^2\exp(-2Kz_0)dk\ , \tag{B15}$$

where

$$k_i^2=\frac{2m_3^*}{\hbar}(V_1-E_i)\ . \tag{B16}$$

If z_0 is sufficiently large so that $Kz_0\gg 1$, the major contribution to the exponential comes from the smallest K, i.e., K_i given by Eq. (B5) with $E=E_i$, and the exponential rapidly decreases as K deviates from K_i. Then, a good approximation to the integral in Eq. (B15) is obtained by approximating the argument in the exponential by its first-order expansion. Calling x the quantity k-k_i we write

$$\int_0^{k_i}k^2\exp(-2Kz_0)dk \approx k_i^2\int_0^{k_i}\exp(-2K_iz_0)\exp\left[-2\frac{k_i}{K_i}z_0x\right]dx \tag{B17}$$

which is easily integrated.

Finally, the transition probability per unit time becomes

$$W=\frac{\hbar}{36m_3^*}\left[\frac{\pi}{2}\right]^5\frac{K_i^2k_i}{K_i^2+k_i^2}\frac{1-\exp(-2k_i^2z_0/K_i)}{z_0} \times\exp(-2K_iz_0)\ . \tag{B18}$$

In the general case, $2k_i^2z_0/K_i$ will be greater than 1 and Eq. (B18) will reduce to

$$W=\frac{\hbar}{36m_3^*}\left[\frac{\pi}{2}\right]^5\frac{K_i^2}{K_i^2+k_i^2}\frac{k_i}{z_0}\exp(-2K_iz_0)\ . \tag{B19}$$

This equation gives a rigorous theoretical expression of the pre-exponential factor in a simple δ function potential limit. Several assumptions must be verified. In the range of interest (deep oxide traps, i.e., $E_i > 0.1$ eV) two of them are always valid: $KL \gg 1$ and $Kz_0 \gg 1$ with z_0 in a range greater than a few Å. The main problem is due to the use of the effective mass approximation especially in the SiO_2 region, but unfortunately it would be a formidable task to go beyond this problem.

APPENDIX C

Now, we introduce the tunneling effect in the calculation of the DLTS response. We start by rewriting Eq. (9) given in the text with the definition of the lock-in correlation function $\Gamma(t)$ given in Appendix A. We have

$$R(T)=R_{it}(T)+A\int_0^{\infty} n_{0t}(E_i,z)J(z)dz\ , \tag{C1}$$

where

$$J(z)=\frac{\pi}{\sqrt{2}P}\left[\int_{P/4}^{P/2}\exp(-e_t\cdot t)dt-\int_{3P/4}^{P}\exp(-e_t\cdot t)dt\right]. \tag{C2}$$

The integrals are easily deduced, and we obtain

$$J(z)=\frac{\pi}{\sqrt{2}Pe_t}\left[\exp(-e_t\cdot P)-\exp\left[-\frac{3}{4}e_t\cdot P\right]-\exp\left[-\frac{e_tP}{2}\right]+\exp\left[-\frac{e_tP}{4}\right]\right]. \tag{C3}$$

This function is similar to the energy window given in Eq. (A14) in the case of interface states. But here we have taken into account the tunneling emission rate $e_t(E_i,z)$ given by Eq. (7). For a given energy barrier E_i, as we have assumed in Sec. III, expression (C3) only depends on the depth z, and $J(z)$ is the probe function with which the DLTS technique analyzes the oxide traps. A computer simulation is given in Fig. 13. This simulation shows that the maximum z_m is given by $\sqrt{E_i}\cdot z_m = 33.26$ with $\alpha = 10^{13}\ s^{-1}$ (with E_i in eV and z_m in Å). This maximum

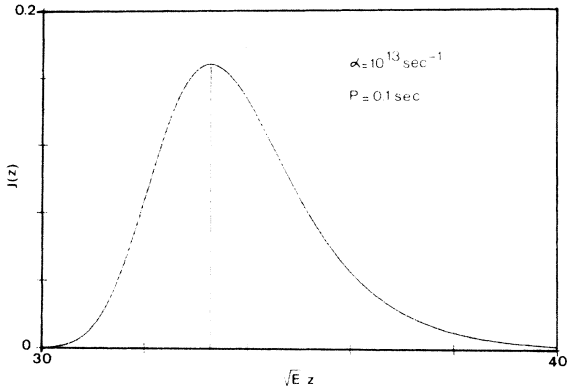

FIG. 13. Plot of the probe function with which the depth analysis of the oxide traps is performed by the DLTS technique.

occurs when the tunneling emission time constant $e_t(E_i,z)$ is equal to the emission time constant window e_{n0} experimentally fixed by the DLTS apparatus: $e_t = e_{n0} = 1.72/P$. Thus, with Eq. (7) we have

$$\sqrt{E_i}\cdot z_m=\frac{\hbar}{2\sqrt{2m_1^*}}\ln\frac{\alpha}{e_{n0}}\ . \tag{C4}$$

The application of this formula agrees very well with the result of the simulation. In this way we have a determination of the localization of the oxide traps.

Then, the DLTS response is obtained by a numerical integration of the probe function $J(z)$. This integration is made by the trapezoidal rule method, and if we assume that $n_{0t}(E_i,z)$ is slowly varying over the range where $J(z)$ is not zero, we obtain the final expression from Eq. (C1):

$$R(T)=R_{it}(T)+0.723\ \text{A}\ n_{0t}(E_i,z_m)\ . \tag{C5}$$

This expression is valid to any values of E_i, α, and P.

It is interesting to note, that this derivation of the DLTS response is similar to the one of interface states. But now the energy spectroscopy is transformed in depth spectroscopy because the tunneling emission rate is strongly depth dependent.

[1] D. V. Lang, J. Appl. Phys. **45**, 3023 (1974).
[2] M. Schultz and N. M. Johnson, Appl. Phys. Lett. **31**, 622 (1977).
[3] M. Schulz and N. M. Johnson, Solid State Commun. **25**, 481 (1978).
[4] N. M. Johnson, D. J. Bartelink, and M. Schulz, in *The Physics of SiO_2 and Its Interface*, edited by S. T. Pantelides (Pergamon, New York, 1978), p. 421.
[5] D. Vuillaume and J. C. Bourgoin, J. Appl. Phys. **58**, 2077 1985.
[6] L. M. Ternan, Solid State Electron. **5**, 285 (1962).
[7] E. H. Nicollian and A. Goetzberger, Bell Syst. Tech. J. **46**, 1055 (1967).
[8] A. Blosse and J. C. Bourgoin, Appl. Phys. **A34**, 1 (1984).
[9] F. P. Heiman and G. Warfield, IEEE Trans. Electron. Devices **ED-12**, 167 (1965).
[10] K. Yamasaki, M. Yoshida, and T. Sugano, Jpn. J. Appl. Phys. **18**, 113 (1979).
[11] D. Pons, Ph.D. thesis, University of Paris VI, 1979.
[12] E. Rosencher and R. Coppard, J. Appl. Phys. **55**, 971 (1984).
[13] N. M. Johnson, Appl. Phys. Lett. **34**, 802 (1979).
[14] N. M. Johnson, J. Vac. Sci. Technol. **21**, 303 (1982).
[15] M. Av-Ron, M. Shatzkes, T. H. Di Stefano, and J. B. Cadoff, in *The Physics of SiO_2 and Its Interface*, Ref. 4, p. 46.
[16] E. H. Nicollian and J. R. Brews, in *MOS Physics and Technology* (Wiley, New York, 1982), pp. 462 and 473.
[17] E. H. Nicollian and J. R. Brews, in *MOS Physics and Technology*, Ref. 16, p. 815.
[18] H. Hasegawa and T. Sawada, J. Vac. Sci. Technol. **16**, 1478 (1979).
[19] H. Preier, Appl. Phys. Lett. **10**, 361 (1967).
[20] B. Balland and P. Pinard, Phys. Status Solidi A **47**, 251 (1978).
[21] A. A. Khan, J. A. Woollam, and Y. Chung, J. Appl. Phys. **55**,

4299 (1984).
[22]D. J. Dimaria, in *The Physics of SiO_2 and Its Interface,* Ref. 4, p. 160.
[23]F. J. Grunthaner *et al.*, J. Vac. Sci. Technol. **16**, 1443 (1979); Phys. Rev. Lett. **43**, 1683 (1979).
[24]J. S. Gradshteyn and I. W. Ryzhik, in *Table of Integrals Series and Products* (Academic, New York, 1965), p. 334.
[25]J. R. Oppenheimer, Phys. Rev. **31**, 66 (1928).